Transient Rheology of a Polypropylene Melt Reinforced with Long Glass Fibers

Ortman, K.C.[1], Neeraj Agarwal[1], D.G. Baird[1] and P. Wapperom[2], Jeffrey Giacomin[3]

Chemical Engineering Department[1], Virginia Tech, Blacksburg, VA 24061
Mathematics Department[2], Virginia Tech, Blacksburg, VA 24061
Mechanical Engineering Department[3], University of Madison-Wisconsin, Madison, WI 53706

Abstract

The purpose of this research is to understand the transient fiber orientation and the associated rheology of long glass fiber (> 1mm) reinforced polypropylene, in a well-defined simple shear flow, in an effort to extend the results and knowledge gained from these fundamental experiments to the use of simulating (more complex) molding processes. Specifically, we are interested in associating the rheological behavior of glass fiber reinforced polypropylene with the transient evolution of fiber orientation in simple shear flow in an effort to ultimately model fiber orientation in complex flow. A sliding plate rheometer was designed to measure stress growth in the startup and cessation of steady shear flow. Results were confirmed by independent measurements on another sliding plate rheometer[13]. Two fiber orientation models were investigated to predict the transient orientation of the long glass fiber system. One model, the Folgar-Tucker model[2,3] (FT), has been particularly useful for short glass fiber[1] systems and was used in this paper to assess its performance with long glass fibers. A second fiber orientation model[8], one that accounts for the flexibility of long fibers as opposed to rigid rod models commonly used for short fibers, was investigated and results are also compared with experimentally measured values of orientation. The accuracy of these models, when used with the stress tensor predictions of Lipscomb[12], is evaluated by comparing the model predictions against experimental stress growth data. Samples consisting of 10% wt. glass fiber in polypropylene with an average fiber length of 4 mm were prepared with random initial orientation and were sheared at different rates. Model predictions show that fiber flexibility has the effect of retarding transient fiber orientation however provides trivial rheological predictions with the chosen stress model. Additionally, it is shown that the predictions of the Folgar-Tucker model are not able to capture the dynamics of neither the orientation evolution nor the stress growth evolution that is measured experimentally.

Introduction

In an effort to produce lightweight energy efficient parts with high moduli, thermoplastics are reinforced with fibers to increase their stiffness, strength, and impact toughness. Such fibers of interest, within this research, are long glass fibers. Currently, glass fiber provides a relatively inexpensive means of producing high strength materials used in energy demanding structures such as automobiles, buildings, and aircraft[9]. Additionally, long glass fibers provide much higher properties, such as Izod Notch Impact (ASTM D256) strength and flexural modulus in the finished part as compared to the same part manufactured with short glass fibers, and are therefore the focus of this research. In this context, term “long” is used to describe a fiber that may exhibit flexibility in the presence of polymer melt flow, whereas “short” fibers will be said to remain rigid under such deformation.

In order to obtain parts with optimum mechanical properties, it is desired to predict fiber orientation and configuration as a function of mold design and processing conditions. Hence, the goal of this work is to understand the dynamic behavior of long glass fibers in a polymer melt flow. Much work has been accomplished in simulating the orientation of short glass fibers in polymeric melts[5,7], however

relatively few efforts have produced applicable models that can be efficiently be used to model long glass fiber orientation. This is, in part, due to the flexible nature of the long glass fibers, whereas short fibers are assumed to be rigid. In this research we explore an orientation model, in a simple shear flow, that takes some aspect of the semi-flexible nature of long fibers into effect. As a basis, we also explore the predictions of the Folgar-Tucker model. We then compare these predictions to experimentally determined results.

Experimental Methods

In this research, the transient startup shear rheology of highly concentrated long glass fibers, in a polypropylene melt, is studied in a sliding plate rheometer. Ten weight percent, 12 mm long glass fibers pellets are extruded and re-pelletized to provide homogeneity. Extrusion does cause fiber breakage. The resulting number average fiber length after extrusion was found to be approximately 4 mm. This material is then compression molded to construct samples of known initial orientation that can be rectilinearly sheared (Figure 1).

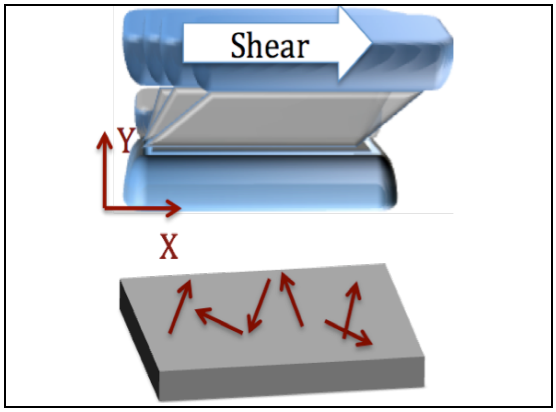

Figure 1: Illustration of a compression molded sample containing planar random initial fiber orientation (below) in a sliding plate apparatus (above).

In this research, samples are subjected to a simple shear flow (Equation 1).

$$v_x(y) = \dot{\gamma}\, y \qquad (1)$$

The transient shear rheology is measured using a shear stress transducer. It is important to note that negligible slipping occurs during the shearing process. This was determined by finding very good agreement between manually measured sample displacements and the automatically measured machine displacements. Using these methods, our mission is to connect the rheology of these materials to their underlying microstructure, specifically fiber orientation.

Fiber orientation, within this research, is experimentally measured using the method proposed by Leeds[6]. This method refers to optically analyzing metallographically polished (microtomed) sample slices (in a plane of interest) and determining the tangential orientation from the resulting ellipse (Figure 2). In general, a surface of the molded sample may have fibers intersecting it from various angles.

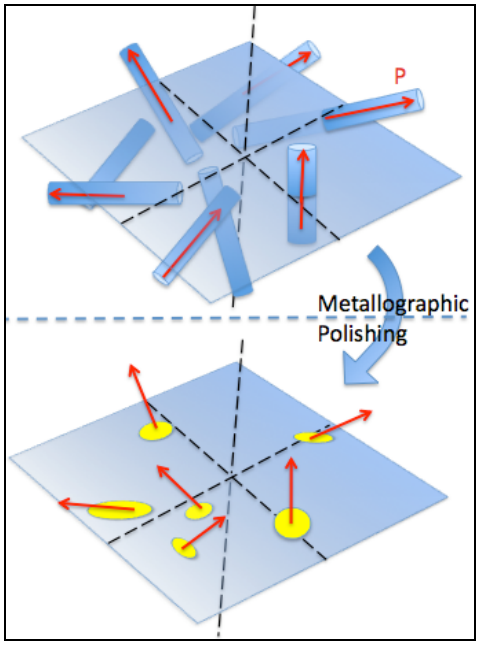

Figure 2: Top: Surface exhibiting fibers with various orientations with respect to the plane. Bottom: Metallographically polished surface exhibiting ellipses.

The orientation with which the fiber intersects the plane is determined by determining the fiber's tangential unit vector from the ellipse image. The word "tangential" is used here because a fiber that exhibits flexibility may have curvature. Hence, we report the orientation with

which a fiber intersects a plane of interest, and average the values over a given thickness. In this paper, orientation data is obtained over the thickness (the 'y' direction in Figure 1) of the polished sample of a sliced plane.

Orientation

Fiber orientation may be predicted by an orientation distribution function[2], $\psi(\vec{p})$, where $\vec{p}$ denotes a unit vector that is parallel to the orientation of a rigid fiber (Figure 3). Here, $\psi(\vec{p})$ represents the probability density of finding a fiber with a specific orientation, and thus may be used to determine average orientation properties. Furthermore, the distribution function is normalized such that its integration over all configurational space is unity. Though completely valid, the orientation distribution function is cumbersome to work with and is usually used to construct an orientation tensor. This can be accomplished by taking the second moment of the orientation vector with respect to the distribution function (Equation 2).

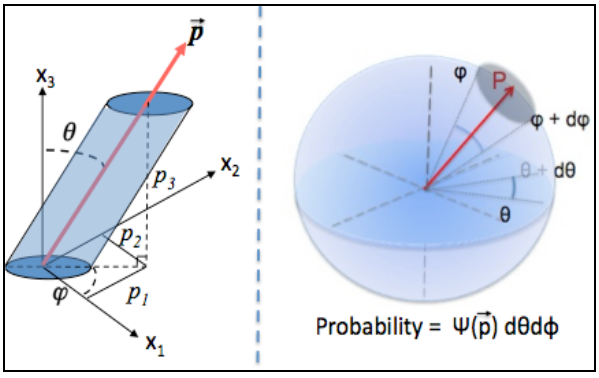

Figure 3: Left: Fiber with unit orientation vector $\vec{p}$. Right: Probability of finding a fiber with the specified orientation.

$$\underline{\underline{A}} = \int \vec{p}\,\vec{p}\,\psi(\vec{p})\,d\vec{p} \qquad (2)$$

$$\underline{\underline{A}}_4 = \int \vec{p}\,\vec{p}\,\vec{p}\,\vec{p}\,\psi(\vec{p})\,d\vec{p} \qquad (3)$$

The orientation tensor provides a measure of the degree of orientation of the fiber in space. Furthermore, the tensor is symmetric and its trace is always equal to unity. Hence, if the A_{11} component is unity ($A_{22} = A_{33} = 0$), then the fiber is fully aligned in the "1" direction. Furthermore, a fourth order orientation tensor (Equation 3) arrives in orientation models as a consequence of the kinematic behavior of the fibers. Numerically, a closure approximation is needed to decouple this tensor into two second order tensors. Our choice of this closure approximation will be mentioned in the next section. Although this development was formulated for rigid fibers, the models in this research will tried to be used to extend the definition of the orientation tensor to flexible fibers by allowing the orientation tensor to describe the tangential orientation of the long fiber.

Models

Now that the tools for quantifying orientation are apparent, a model is needed to explain its dependence within a flow field. Both the Folgar-Tucker[2] model and Bead-Rod model, suggested by Strautins and Latz[7], will be used with the stress predicting Libscomb model to fit model parameters that are most consistent with both the measured orientation evolution and the transient rheology. The accuracy of the models is then discussed.

Folgar-Tucker Model

The Folgar-Tucker model, which has seen much use since its introduction in the 1980's, was developed for short glass fibers in the concentrated regime. Here, the term concentrated is used to describe the ability for significant fiber-fiber interactions to occur. The model has been developed to extend Jeffery's model, introduced in the 1920's, by introducing an isotropic rotary diffusion term. This term, called the Folgar-Tucker term, inhibits the steady state alignment of the fibers from being fully oriented (Equation 4).

$$\frac{D\underline{\underline{A}}}{Dt} = \underbrace{\underline{\underline{A}}\cdot\underline{\underline{\kappa}}^T + \underline{\underline{\kappa}}\cdot\underline{\underline{A}} - [(\underline{\underline{\kappa}} + \underline{\underline{\kappa}}^T):\underline{\underline{A}}]\underline{\underline{A}}}_{\text{Generalized Jeffery for Fibers}} + \underbrace{2C_I II_D(\underline{\underline{\delta}} - 3\underline{\underline{A}})}_{\text{Folgar-Tucker Term}} \quad (4)$$

Within this model, D/Dt is the material derivative, $\underline{\underline{\kappa}}^T$ is the velocity gradient tensor whose i,jth component is defined as $\partial v_j / \partial x_i$, and C_I is the isotropic rotary diffusion term, II_D is the second invariant of the rate of strain tensor ($\underline{\underline{D}}$) defined as $\underline{\underline{D}} = \frac{1}{2}\left(\underline{\underline{\kappa}} + \underline{\underline{\kappa}}^T\right)$, and $\underline{\underline{\delta}}$ is the unit tensor. For the simulation of this model, the quadratic closure approximation is used to decouple to the fourth order orientation tensor.

$$\underline{\underline{A}}_4 = \underline{\underline{A}}\,\underline{\underline{A}} \text{ (quadratic closure approx.)} \quad (5)$$

Because our fibers are long, we wish to explore a model that attempts to account for flexibility.

Bead Rod Model

The model being referred to here was published in 2007 by Strautins and Latz[8]. This Bead Rod model (BR) was published as a continuum fiber model for dilute solutions that provides a first approximation to flexibility. This is accomplished by modeling a fiber as two rods connected by a pivot allowing bead (Figure 4).

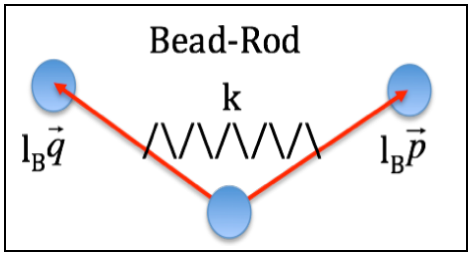

Figure 4: Fiber model, with segment length l_B, allowing semi-flexibility. The segment orientations are denoted by unit vectors $\vec{p}$ and $\vec{q}$, and resist bending by some spring constant k.

The model constructs two rigid segments with length l_B that are allowed to slightly pivot about the connecting bead, with some restorative spring rigidity k. Both $\vec{p}$ and $\vec{q}$ are unit vectors that represent the orientation of the corresponding fiber segments, with respect to the center bead. Although specifically derived for small bending angles, $\vec{q} \cong -\vec{p}$, we will ignore this restriction in simple shear flow due to the fact that no interesting information is gained from this model otherwise. This is due to the fact that this model predicts flow induced bending only in complex flows, and not simple flows. However, if the fibers have a good degree of initial bending to them, they can exhibit some behavior in simple flows, as will be discussed below. Additional assumptions used in this development state that the fiber has negligible inertia, inferring that the center of mass of the fiber instantaneously adjusts to changes in solvent velocity, and lastly that the fiber is neutrally buoyant within the suspending medium. The kinematics and governing Smoluchowski equation are developed for the representative fiber and used to form the following model (Equations 6-9),

$$\begin{aligned}\frac{D\underline{\underline{A}}}{Dt} &= \underline{\underline{A}}\cdot\underline{\underline{\kappa}}^T + \underline{\underline{\kappa}}\cdot\underline{\underline{A}} - [(\underline{\underline{\kappa}} + \underline{\underline{\kappa}}^T):\underline{\underline{A}}]\underline{\underline{A}} \\ &\ldots + \frac{l_B}{2}[\vec{C}\vec{\mu} + \vec{\mu}\vec{C} - 2(\vec{\mu}\cdot\vec{C})\underline{\underline{A}}] \\ &\ldots - 2k[\underline{\underline{B}} - \underline{\underline{A}}\,tr(\underline{\underline{B}})]\end{aligned} \quad (6)$$

$$\begin{aligned}\frac{D\underline{\underline{B}}}{Dt} &= \underline{\underline{B}}\cdot\underline{\underline{\kappa}}^T + \underline{\underline{\kappa}}\cdot\underline{\underline{B}} - [(\underline{\underline{\kappa}} + \underline{\underline{\kappa}}^T):\underline{\underline{A}}]\underline{\underline{B}} \\ &\ldots + \frac{l_B}{2}[\vec{C}\vec{\mu} + \vec{\mu}\vec{C} - 2(\vec{\mu}\cdot\vec{C})\underline{\underline{B}}] \\ &\ldots - 2k[\underline{\underline{A}} - \underline{\underline{B}}\,tr(\underline{\underline{B}})]\end{aligned} \quad (7)$$

$$\begin{aligned}\frac{D\vec{C}}{Dt} &= \underline{\underline{\kappa}}\cdot\vec{C} - (\underline{\underline{A}}:\underline{\underline{\kappa}})\vec{C} + \frac{l_B}{2}[\vec{\mu} - \vec{C}\left(\vec{\mu}\cdot\vec{C}\right)] \\ &\ldots - k\vec{C}[1 - (tr(\underline{\underline{B}})]\end{aligned} \quad (8)$$

$$\vec{\mu} = \sum_{i=1}^{3}\left(\sum_{j=1}^{3}\sum_{k=1}^{3}\frac{\partial^2 v_i}{\partial x_i \partial x_k}A_{jk}\right)\vec{e}_i \quad (9)$$

where the two orientation tensors ($\underline{\underline{A}}$ and $\underline{\underline{B}}$) represent the second moment of the orientation

distribution function with respect to the unit vectors, $\vec{p}$ and $\vec{q}$, in the following manner:

$$\underline{\underline{A}} = \int \vec{p}\,\vec{p}\,\psi(\vec{p},\vec{q})\,d\vec{p}\,d\vec{q} \tag{10}$$

$$\underline{\underline{B}} = \int \vec{p}\,\vec{q}\;\psi(\vec{p},\vec{q})\,d\vec{p}\,d\vec{q} \tag{11}$$

As a direct consequence of the bending rigidity, encompassed within the model parameter *k*, the expectancy of a segment's orientation (with respect to the orientation distribution function) may be non-zero in general, and is accounted for in (Equation 12) by the following definition:

$$\vec{C} = \int \vec{p}\,\psi(\vec{p},\vec{q})\,d\vec{p}\,d\vec{q} \tag{12}$$

Lastly, (Equation 9) contributes the effects of flow-induced fiber bending from the presence of second order derivatives of the velocity field (as mentioned previously). In simple flows, for example, all components are *0*, and no flow-induced fiber bending is predicted to occur. Equation 9 is a vector and has at most three components, each denoted by a unit directional vector (dyad) $\vec{e}_i$.

In simple shear flow, this model is reduced significantly due to the non-existence of second order velocity derivatives. Additionally, we can adapt the isotropic rotary diffusion term of Folgar and Tucker in an ad-hoc manner to probe concentrated suspensions (Equation 13 and 14).

$$\frac{D\underline{\underline{A}}}{Dt} = \underline{\underline{A}}\cdot\underline{\underline{\kappa}}^T + \underline{\underline{\kappa}}\cdot\underline{\underline{A}} - [(\underline{\underline{\kappa}} + \underline{\underline{\kappa}}^T) : \underline{\underline{A}}]\underline{\underline{A}} \\ \ldots - 2k[\underline{\underline{B}} - \underline{\underline{A}}\;tr(\underline{\underline{B}})] - 6C_I\dot{\gamma}\left(\underline{\underline{A}} - \frac{1}{3}\underline{\underline{\delta}}\right) \tag{13}$$

$$\frac{D\underline{\underline{B}}}{Dt} = \underline{\underline{B}}\cdot\underline{\underline{\kappa}}^T + \underline{\underline{\kappa}}\cdot\underline{\underline{B}} - [(\underline{\underline{\kappa}} + \underline{\underline{\kappa}}^T) : \underline{\underline{A}}]\underline{\underline{B}} \\ \ldots - 2k[\underline{\underline{A}} - \underline{\underline{B}}\;tr(\underline{\underline{B}})] - 6C_I\dot{\gamma}\left(\underline{\underline{B}} - \frac{tr(\underline{\underline{B}})}{3}\underline{\underline{\delta}}\right) \tag{14}$$

The physical interpretation of the $\underline{\underline{A}}$ tensor is that it describes the orientation tensor of a given rod, either $\vec{p}$ or $\vec{q}$. The $\underline{\underline{B}}$ tensor, on the other hand, describes the end-to-end distance between the two rods at any given time and thus, in simple flows where no second order velocity gradients exist, behaves as a time delay for the model fiber to "open" (provided it has some initial bending to it). To take advantage of this time delayed effect, we wish to phenomenologically choose to use an orientation tensor constructed from the dimensionless end-to-end vector (Equation 15), (Figure 5). This choice will give us a little more control over the dynamics of the orientation evolution.

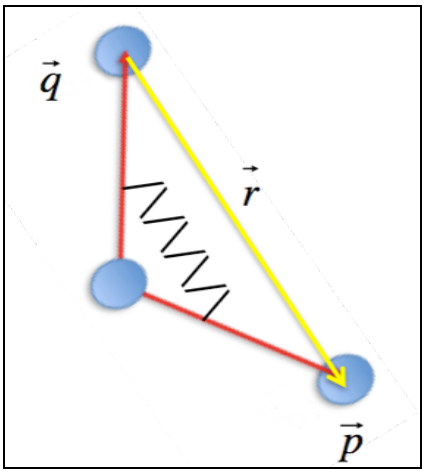

Figure 5: Illustration of the dimensionless end-to-end vector of a bead-rod model fiber.

$$\vec{r} = \vec{p} - \vec{q} \qquad (15)$$

Using this definition of the end-to-end vector, an analogous definition of the orientation tensor (constructed from the end-to-end vector) can be formed by taking the second moment of this vector with respect to the orientation tensor (Equation 16).

$$\underline{\underline{rr}} = \int \vec{r}\vec{r}\, \psi(\vec{p},\vec{q},t) d\vec{p}\, d\vec{q} \qquad (16)$$

This form of the orientation tensor is not fully useful because it has not yet been normalized. Hence, the normalized form of this tensor is obtained by dividing the tensor by the magnitude of the end-to-end vector. This is equivalent to normalizing the tensor with respect the trace of this tensor to form (Equation 17).

$$\underline{\underline{R}} = \frac{\underline{\underline{rr}}}{tr(\underline{\underline{rr}})} \text{(normalized end-to-end tensor)} \qquad (17)$$

Libscomb Stress Model

The Libscomb stress model will be used in this research to relate the transient fiber orientation within the melt to the transient viscosity behavior of the suspension. The quadratic closure approximation will again be used. Again, the orientation representation used in this model will be of the end-to-end form (Equation 17). With this adaptation, the Libscomb model[12] for the transient shear viscosity (η^+) becomes (Equation 18).

$$\eta^+ = \eta_s + c_1 \varphi \eta_s + 2\varphi \eta_s N R_{12}^2 \qquad (18)$$

In this expression, η_s is the neat matrix viscosity, φ is the volume fraction of fibers, c_1 is a coefficient responsible for the viscosity enhancement due to the presence of fibers, N is a parameter associated with the enhancement due to fiber orientation, and R_{12} is the 1-2 component of the orientation tensor. It is worth mentioning, for the case of Folgar-Tucker, that the orientation tensor ($\underline{\underline{A}}$) of a rigid rod is the same as its end-to-end orientation ($\underline{\underline{R}}$) because a rigid rod doesn't bend. For concentrated suspensions, both c_1 and N are fit parameters for this stress model. With this description, it is apparent that the second term provides viscosity enhancement due to the presence of fibers, and the third term represents enhancements from fiber orientation changes. One will note that this model does not account for shear thinning, however shear thinning is very common in the rheology of nonNewtonian fluids, such as those in this research.

Results

Extruded long glass fiber strands (with a post-extruded average fiber length of 4 mm) were given an initially random planar orientation and sheared for 70 strain units at shear rates of 0.4, 1.0, and 4.0 sec^{-1}. The transient rheologies of the fiber suspensions are shown in (Figure 6).

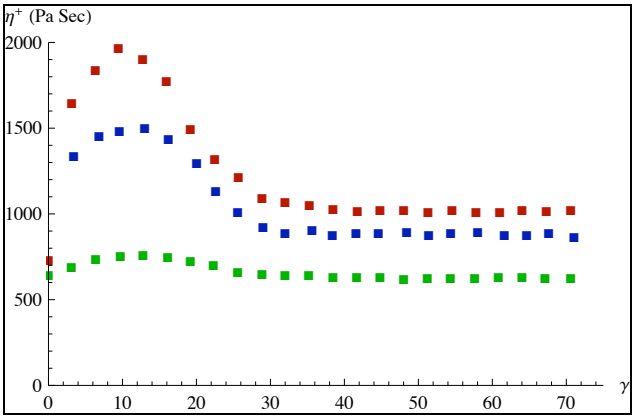

Figure 6: Experimentally measured transient viscosity vs. strain for 10% long glass fibers initially oriented randomly in the shear plane, at various shear rates [■=0.4 sec^{-1}, ■=1.0 sec^{-1}, ■=4.0 sec^{-1}]

As one can see, the shear stress overshoot are larger at lower shear rates. Likewise, shear thinning is also visible. These effects have been reported in literature and have been said to be due to long fiber flocculation[14]. At higher shear rates, the aggregates are more easily broken and

hence lower peaks and steady state viscosities are realized. The corresponding orientation evolution at 1.0 sec^{-1} is depicted in (Figure 7).

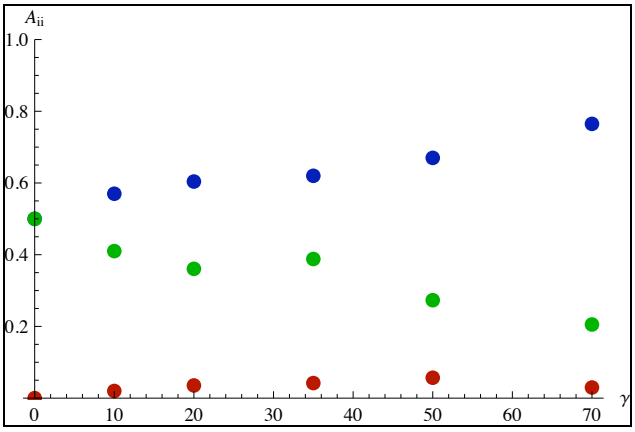

Figure 7: Experimentally determined data for the orientation evolution of the trace components of the orientation tensor versus strain at a shear rate of 1.0 sec^{-1}. System is 10% wt. glass fibers initially random in shear plane. [Data=Points, ●=A_{11}, ●=A_{22}, ●=A_{33}]

Using this orientation information, the orientation model parameters can be fit. Initial conditions of the orientation models for planar random fibers are $A_{11}=A_{33}=1/2$, $A_{ij\neq 11,33}=0$, and $B_{ij}=0$. These conditions infer that the end-to-end orientation tensor has the initial conditions of $R_{11}=R_{33}=1/2$, $R_{ij\neq 11,33}=0$. One disadvantage of the Folgar-Tucker model is that the orientation kinetics cannot be slowed down. This is untrue for the relatively new 'Reduced Strain Closure' model of Tucker, et al.[15], however this form will not be evaluated in this paper. Using the original form of the Folgar-Tucker model, the isotropic rotary diffusion coefficient (C_I) may be fit to obtain the largest strain value of orientation given in (Figure 7). Ideally, this value should conform to the steady state value of the transient orientation, but the data at 70 strain units shown in (Figure 7) is the closest value available to the true steady state orientation. This same value will also used in the Bead Rod model, however k may be varied to either slow or speed up the orientation kinetics, in this situation. It is very important to reiterate the distinction between these two models again. The Bead Rod model was used in this paper to slow orientation kinetics by giving the fibers a random in-plane orientation, identical to that used by the Folgar-Tucker model, but also with a random initial bending angle (not found in rigid rod theory such as the

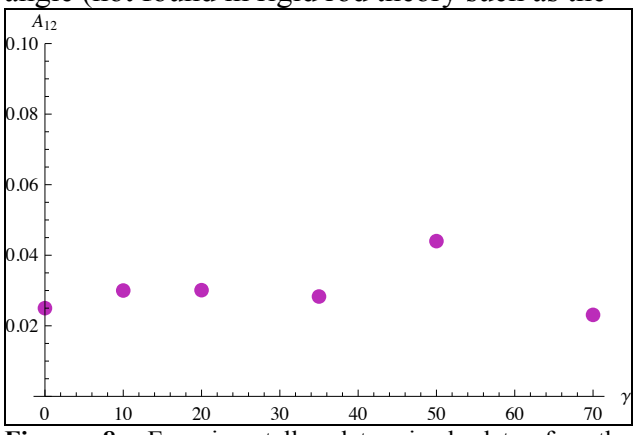

Figure 8: Experimentally determined data for the orientation evolution of the 1-2 component of the orientation tensor versus strain at a shear rate of 1.0 sec^{-1}. System is 10% wt. glass fibers initially random in shear plane. [Data=Points, ●=A_{12}]

Folgar-Tucker model). This allows the restorative spring rigidity k to be varied and behave as a time delayed orientation parameter, as mentioned before. The isotropic rotary diffusion term was found to be CI = 0.038 to asymptotically approach the largest strain value of orientation available. Using a least squared error method, the bending rigidity term of the Bead-Rod model was determined to be k=0.012. Using these parameters, the orientation model predictions can be compared with the experimentally determined values (Figure 9).

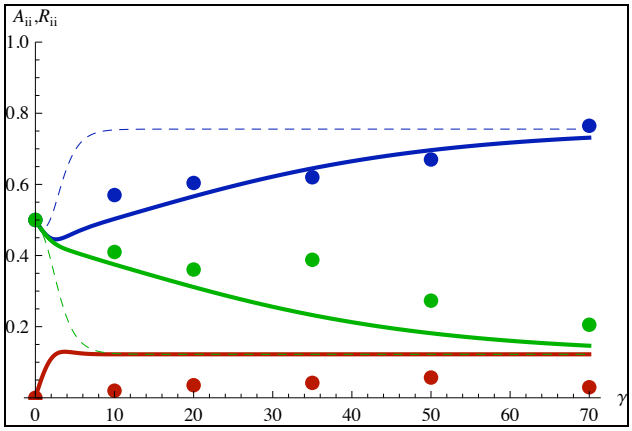

Figure 9: Experimentally determined data and model predictions for the orientation evolution of the trace components of the orientation tensor (A_{ii} for Folgar-

Tucker and Data, and R_{ii} for the Bead Rod model) versus strain at a shear rate of 1.0 sec^{-1}. System is 10% wt. glass fibers initially random in shear plane. C_I=0.038, k =0.012. [Data=Points, FT=Dashed, BR=Solid, ●=A_{11},R_{11}, ●=A_{22},R_{22}, ●=A_{33},R_{33}]

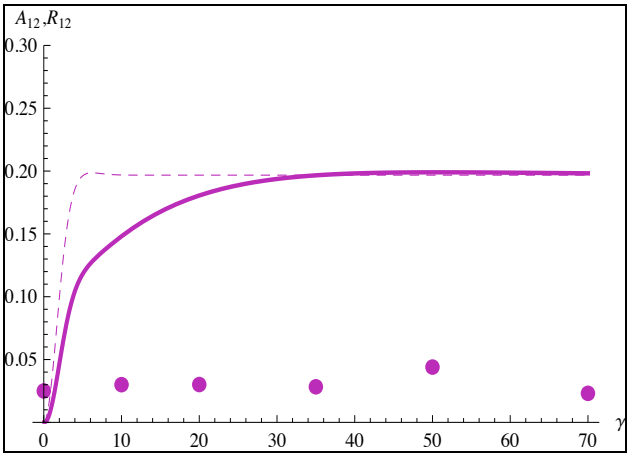

Figure 10: Experimentally determined data and model predictions for the orientation evolution of the 1-2 component of the orientation tensor (A_{12} for Folgar-Tucker and Data, and R_{12} for the Bead Rod model) versus strain at a shear rate of 1.0 sec^{-1}. System is 10% wt. glass fibers initially random in shear plane. C_I=0.038, k =0.012. [Data=Points, FT=Dashed, BR=Solid, ●=A_{12},R_{12}]

As one can see from (Figures 9 and 10), the Folgar-Tucker model over predicts the rate of orientation. The Bead-Rod model, on the other hand, approaches the predictions of the Folgar-Tucker more slowly. One important difference is apparent in (Figure 10). The models' values of the 1-2 component of the orientation tensor converge in (Figure 10), but the Bead-Rod model shows no overshoot. This is especially apparent when the orientation models are used in combination with the Libscomb model to predict the transient stress growth (Figure 11).

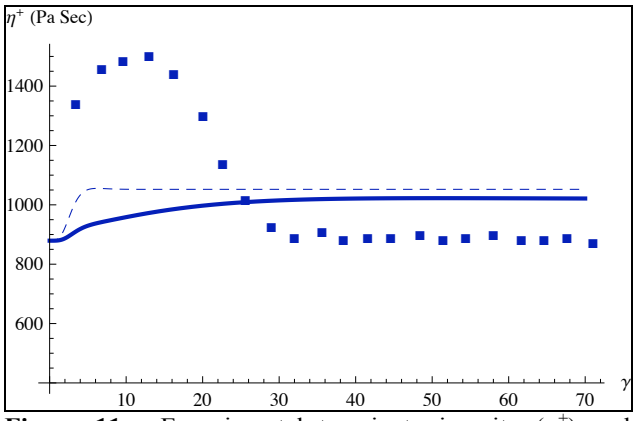

Figure 11: Experimental transient viscosity (η^+) and model fits (using the orientation models in combination with the stress Libscomb model) for fibers initially random in plane and sheared at 1.0 sec^{-1}. [■=1.0 sec^{-1}, Data=Points, FT=Dashed, BR=Solid]. [Model Parameters for FT: C_I=0.038, c1=15, N=105. Model Parameters for BR: C_I=0.038, k=0.012, c_1=15, N=85].

For the 10% wt. glass fiber systems of interest, the volume fraction of fiber is φ=0.038, and the neat polyproplene matrix viscosity is η_s=560 Pa*sec at a shear rate of 1.0 sec^{-1}. The stress model parameters (c_1 and N), in combination with the orientation models and their respective model parameters already determined from the transient orientation data, were also determined by using a minimized error approach. Despite the small viscosity overshoot predicted by using the Folgar-Tucker model (in combination with the stress model), it is not able to capture the magnitude of the overshoot. The Bead Rod model, on the other hand, does not show even a slight overshoot prediction and overall produces a rather trivial and useless viscosity profile. Additionally, when the Bead Rod model, and its parameters that were determined from one set of data, are used to predict the orientation evolution and corresponding rheology at a shear rate of 4.0 sec^{-1}, it produces results that are further incorrect. Specifically, the orientation versus strain profile is predicted to be even slower than what was fit at 1.0 sec^{-1}. This is because the delay in orientation is based on time and not strain, thus effectively retarding the orientation evolution even more drastically. This is incorrect because, although not shown in this paper, experimentally we see fibers align more quickly at higher shear rates. Again, this

retardation completely eliminates the prediction of a viscosity overshoot and hence provides a particularly poor understanding of the rheology. It is apparent from this treatment that neither of these orientation models can be used with the stress model chosen to accurately relate the transient rheology with the underlying fiber orientation.

Summary and Conclusion

An orientation model that tries to account for flexibility was used with the stress predicting Libscomb model to try to link the rheological behavior of long glass fiber reinforced polypropylene to its fiber orientation microstructure. Additionally, the much more widely acknowledged Folgar-Tucker model was also used as a standard for comparison. Orientation model parameters were fit from transient orientation data, and stress model parameters were fit from simple shear flow rheology, both at a shear rate of 1.0 sec^{-1}. It was shown that the orientation and stress models used in this paper are not fully consistent with experimentally determined values. This is apparent in the lack of ability of either model to accurately capture the dynamics of the measured transient rheology. Additionally, the Bead Rod model, when used in the manner describe by this paper, predicts slower orientation kinetics at higher shear rates that are in contradiction with both experiment and intuition. It may seem, at this point, that in simple flows the use of the Bead Rod model provides a rheological disadvantage over the Folgar-Tucker model, but a better stress model may simply be needed to understand long fiber rheology. The fundamental goal of this research is to accurately predict complex flow processes (ie. molding processes), but a better combination of orientation and stress model is still needed for the fiber system of interest (ie. concentrated long glass fiber reinforced thermoplastics). A correct combination of orientation and stress model is not found in this research.

Acknowledgments

Financial of NSF/DOE: DMI-0853537

References

1. Eberle, A., et al., *J. Rheol.* **53**, 685-706 (2008).
2. Advani, S.G., and Tucker III, C.L., *J. Rheol*. **31**, 751-84 (1987).
3. Advani S.G. and Tucker III C.L., *J. Rheol*. **34,** 367-386 (1990).
4. Baird D. G. and Collias, D. I., Polymer Processing, Boston: Butterworth-Heinemann, 1998.
5. Folgar, F. P. and Tucker III, C. L., *J. Reinf. Plast. Comp.* **3**, 98-119 (1984).
6. Hine, P.J., Davidson, N., Duckett, R.A., *Poly. Comp.* **17**, 720–729 (1996).
7. Bay R. S. and Tucker III, C. L., *Polym Eng Sci.* **32**, 240-253 (1992).
8. Strautins, U. and Latz,A., *Rheol. Acta.* **46**. 1057-1064 (2007).
9. Smith, W. and Hashemi, J., Foundations of Material Science and Engineeering. *McGraw Hill* (2006)
10. Junke, X. and Costeux, S., *Rheo. Acta.* **46**, 815-824 (2007).
11. Velez-Garcia, G., Ortman K., *ICOR Conf. Proc.* **1027**, 42-44 (2008).
12. Lipscomb, G., et al., *J. Non-Newt. Fluid. Mech*. **26**, 297–325 (1988).
13. Kolitawong, C. and Giacomin, A.J., J. Non-Newt. Fluid. Mech. **102**, 71-96 (2002).
14. Keshtkar, M., et al., J. Rheol., 2009. 53: p. 631-650.
15. Wang, J., O'Gara, J., and Tucker III, C. L., *J. Rheol.* **52**(5), 1179-1200 (2008).

Key Words: Long glass fiber rheology, long glass fiber orientation, sliding plate rheometer, flexible fiber, composite, glass reinforced thermoplastic